

INPOP NEW RELEASE: INPOP19a

A. Fienga^{1,2}, V. Viswanathan^{2,3}, P. Deram¹, A. Di Ruscio^{4,1}, L. Bernus^{2,1},
J. Laskar², M. Gastineau², N. Rambaux², O. Minazzoli⁵, D. Durante⁴, L. Iess⁴

¹ Géoazur-CNRS 7329, Université Côte d'Azur, Observatoire de la Côte d'Azur,
France - agnes.fienga@oca.eu

² IMCCE, CNRS, PSL University, Observatoire de Paris - France

³ Goddard Space Flight Center, Greenbelt - USA

⁴ Department of Mechanical and Aerospace Engineering, Sapienza University - Italy

⁵ Artemis, CNRS, Université Côte d'Azur, Observatoire de la Côte d'Azur - France

ABSTRACT. We present here the new planetary ephemeris INPOP19a for the orbits of the 8 planets of the solar system, the moon, Pluto as well as 14000 asteroids. It is fitted over about 155000 planetary observations including 9 positions of Jupiter deduced from the Juno mission, an extension of the Cassini data sample from 2014 to 2017 for the Saturn orbit and of the MEX data from 2016.4 to 2017.4 for the Mars orbit. The asteroid orbits were fitted on the almost 2 millions of observations obtained by the GAIA mission and delivered with the DR2. Finally a new bayesian procedure for the computation of the masses of 343 main-belt asteroids has been applied and leads to an important improvement in the accuracy of the Mars orbit and of its extrapolation capabilities. INPOP19a is available on www.imcce.fr/inpop.

1. INPOP19A : THE NEW PLANETARY EPHEMERIDES

1.1 Update of the data sample In this new ephemeris, the nine first perijove of Juno around Jupiter have been included improving the accuracy of the Jupiter barycentric orbit. Furthermore with the end of the Cassini mission in 2017, a new analysis of the data used for the navigation and for the radio experiment was proposed in order to benefit from the best knowledge in terms of gravity field and Cassini orbital systematics accumulated over the mission duration. In this context, new positions deduced from an independent analysis of Cassini data were obtained and taken into account into the INPOP construction, extending the time coverage for the Cassini data sample from 2014 to 2017. The full dataset used for the INPOP19a adjustment is presented in Table ???. In this table are given the periods of each data sample as well as the number of observations and their average accuracies. The last two columns give the weighted root mean square (WRMS) for each data sample estimated with INPOP19a and INPOP17a.

1.2 Postfit residuals and comparison to INPOP17a

The last two columns of Table ??? give the WRMS of the post-residuals obtained for INPOP19a and INPOP17a. As it can be seen the improvement is clear for Jupiter, Saturn and Mars.

For Mars, as explained in section ??? and in (Fienga et, 2019), the gain in postfit residuals is significant, in particular for the MRO/MO residuals and is due to i) an improvement in the solar plasma correction ii) and mainly to a new method for constraining asteroid masses perturbing the Mars orbits. For MRO/MO, INPOP19a improves INPOP17a residuals by 44% on a common interval of fit.

For Jupiter the improvement is obviously brought by the Juno tracking data. It reaches 2 order of magnitude: from about 2 km for INPOP17a to 20 m for INPOP19a in keeping good residuals for the other flybys obtained between 1975 to 2001.

For Saturn, the prolongation of the data set from 2014 to 2017 was crucial to identify the

Table 1: INPOP19a data samples used for its adjustment. The columns 1 and 2 give the observed planet and an information on the source of the observations. Columns 3 and 4 provide the number of observations and the time interval, while the column 5 gives the *a priori* uncertainties provided by the space agencies or the navigation teams. Finally in the last two columns, are given the WRMS for INPOP19a and INPOP17a.

Planet / Type	#	Period	Averaged Accuracy	WRMS	
				INPOP19a	INPOP17a
Mercury					
Direct range [m]	462	1971.29 : 1997.60	900	0.95	0.96
Messenger range [m]	1096	2011.23 : 2014.26	5	0.82	1.29
Mariner range [m]	2	1974.24 : 1976.21	100	0.37	0.78
Venus					
VLBI [mas]	68	1990.70 : 2013.14	2.0	1.13	1.178
Direct range [m]	489	1965.96 : 1990.07	1400	0.98	0.98
Vex range [m]	24783	2006.32 : 2011.45	7.0	0.93	0.93
Mars					
VLBI [mas]	194	1989.13 : 2013.86	0.3	1.26	1.16
Mex range [m]	30669	2005.17 : 2017.37	2.0	0.98	3.37
		2005.17 : 2016.37	2.0	0.97	1.26
MGS range [m]	2459	1999.31 : 2006.70	2.0	0.93	1.31
MRO/MO range [m]	20985	2002.14 : 2014.00	1.2	1.07	1.91
Jupiter					
VLBI [mas]	24	1996.54 : 1997.94	11	1.01	1.03
Optical ra/de [arcsec]	6416	1924.34 : 2008.49	0.3	1.0	1.0
Flybys ra/de [mas]	5	1974.92 : 2001.00	4.0/12.0	0.94/1.0	0.58/0.82
Flybys range [m]	5	1974.92 : 2001.00	2000	0.98	0.71
Juno range [m]	9	2016.65 : 2018.68	20	0.945	116.0
Saturn					
Optical ra/de [arcsec]	7826	1924.22 : 2008.34	0.3	0.96/0.87	0.96/0.87
Cassini					
VLBI ra/de [mas]	10	2004.69 : 2009.31	0.6/0.3	0.97/0.99	0.92/0.91
JPL range [m]	165	2004.41 : 2014.38	25.0	0.99	1.01
Grand Finale range [m]	9	2017.35 : 2017.55	3.0	1.14	29.0
La Sapienza range [m]	614	2006.01 : 2016.61	6.0	1.01	2.64
Uranus					
Optical ra/de [arcsec]	12893	1924.62 : 2011.74	0.2/0.3	1.09 / 0.82	1.09 / 0.82
Flybys ra/de [mas]	1	1986.07 : 1986.07	50/50	0.12 / 0.42	0.42 / 1.23
Flybys range [m]	1	1986.07 : 1986.07	50	0.92	0.002
Neptune					
Optical ra/de [arcsec]	5254	1924.04 : 2007.88	0.25/0.3	1.008 / 0.97	1.008 / 0.97
Flybys ra/de [mas]	1	1989.65 : 1989.65	15.0	0.11 / 0.15	1.0/1.57
Flybys range [m]	1	1989.65 : 1989.65	2	1.14	1.42

contribution of TNOs into the perturbations to be applied on the Saturn orbit. Furthermore the introduction of data obtained between 2006 and 2016 and analyzed independently from JPL is also very important to confirm that these data obtained in between 2006 and 2007 have to be taken into account in the adjustment with a high level of weighting. The improvement between INPOP17a and INPOP19a is of a factor 30 for the Grand Finale and 2.6 for the period between 2006 and 2016.

2. ASTEROID MASSES

As described in (Fienga et, 2019), we combine knowledge of the physical properties of asteroids by spatial or ground-based surveys, in particular spectral classes, to planetary ephemerides determinations of masses in order to enlarge the set of estimated asteroid masses and study their consistency with the spectral classes of the asteroids. For the mass determination, we use a constrained least square method based on the BVLS (Bounded Values Least Squares) algorithm from (Lawson and Hanson, 1974) which limits the fitted parameters to given intervals. Bounds have been selected according to the parameters of the fit: for asteroid masses, the lower bounds and the upper bounds are chosen according to the *a priori* masses and the *a priori* uncertainties deduced from the literature. The selection of 343 asteroids perturbing the planetary orbits is done based on the method of (Kuchynka and Folkner, 2014) and (Folkner et al. 2014). For defining the bounds, we separate the sample in the three taxonomic complexes C, S, and X according to the spectral informations extracted from the M3PC data base (`mp3c.oca.eu`). *A priori* uncertainties on the initial guess values for the masses are deduced by considering random sampling of the density uncertainties and by including the $3\text{-}\sigma$ diameter uncertainties to the density lower bounds and the upper bounds. A detailed description of the method is given in (Fienga et, 2019). In Figure ?? are compared the densities obtained with INPOP19a and those deduced from INPOP17a and DE430. As one can see, the INPOP19a density distribution is far more realistic : when INPOP17a and DE430 may obtained densities up to several tens of g.cm^{-3} , the maximum density obtained with INPOP19a is of about 6 g.cm^{-3} . Furthermore the INPOP19a distribution in term of taxonomic complexes is also closer from expected than the one of INPOP17a and DE430. At the end 103 asteroids have their masses determinated with INPOP19a with an accuracy better than 30 %.

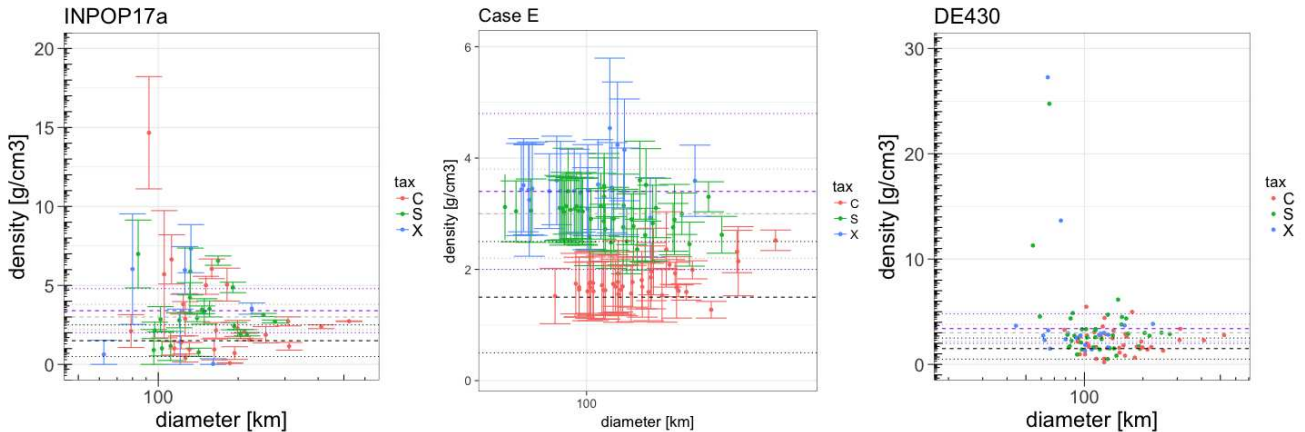


Figure 1: Comparisons between INPOP19a (Case E), INPOP17a and DE430. The x-axis gives the diameters in kilometers and y-axis indicates the densities in g.cm^{-3} .

3. GAIA DR2 ASTEROID ORBITS

In 2013, was launched the astrometric satellite GAIA. Among observations of about 1 billion of stars with an accuracy down to $24 \mu\text{arcseconds}$, the satellite also observed objects in the solar system. In 2018, were released positions and velocities of about 14 099 known Solar System objects

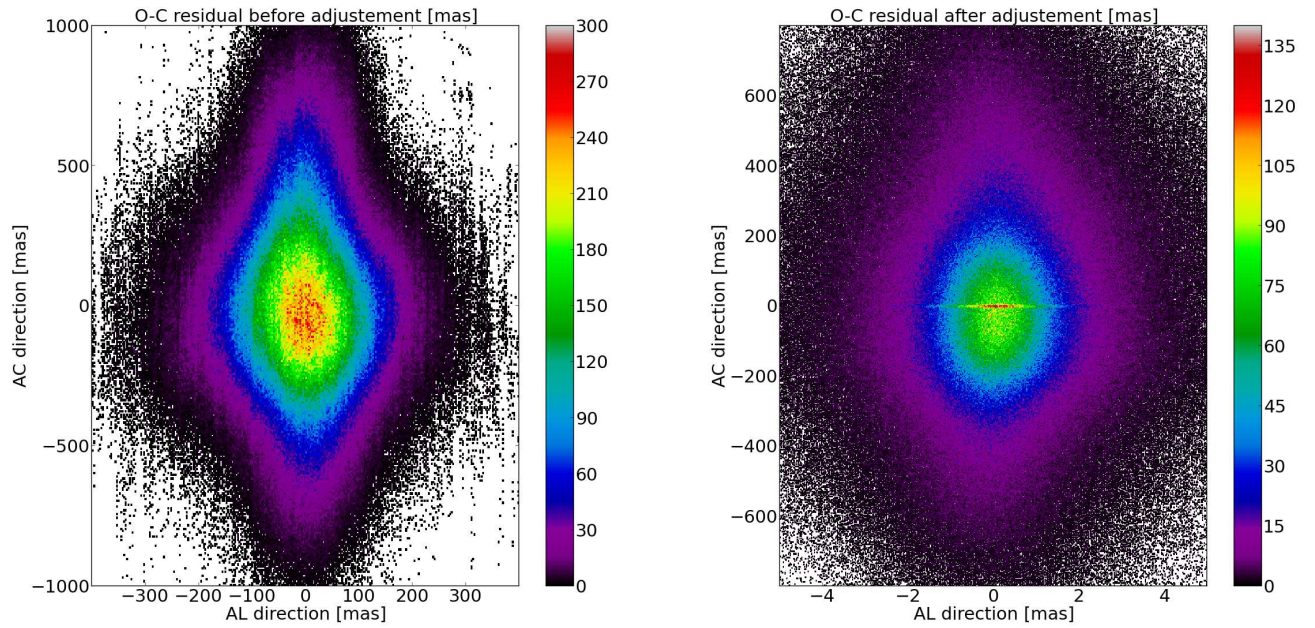


Figure 2: Density plot of the residuals in the (AL,AC) plane given in mas before and after the adjustment of the initial conditions. The colorbar and the axis range were chosen to be directly comparable with Figure 19 of (Gaia collaboration, 2018)

mainly main belt, Near-Earth and Kuiper belt asteroids based on nearly 2 millions observations. The positions were acquired in the GAIA specific coordinates AL and AC as described in (Gaia collaboration, 2018) with an optimal range of brightness $G=12-17$ where the accuracy in the AL-direction reaches the milliarcsecond (mas). As the error on AC remains considerably larger, the information provided by GAIA is essentially one dimensional. These particular features give rise to very strong correlations between right ascension and declination coordinates given in the barycentric reference system (BCRS) and have to be fully taken into account during the orbit determination process. 14099 orbits have then been integrated with INPOP together with the planetary and moon orbits. We fit these orbits to the GAIA data in using the correlation matrix provided by the DPAC. We did not fit the planetary orbits together with the asteroid orbits but we iterate the procedure in order to include the asteroid orbital improvements brought by the GAIA observations to the computation and the adjustment of the planet orbits. In order to integrate the motion of 14099 orbits in a reasonable time, we included the perturbations of the Sun and of the main planets but in a newtonian formalism and in taking into account only a reduced number of the biggest asteroids that can have an influence on the other asteroid orbits. For a sake of comparison, we chose the same list of perturbing asteroids (16) as in (Gaia collaboration, 2018). However, after testing different alternative lists of perturbers, due to the limited interval of time covered by the GAIA data (22 months), no differences are noticeable on the residuals after the fit. Figure ?? presents the residuals obtained before and after the fit of the 14099 asteroids in using INPOP19a. The obtained results are very similar to those published by (Gaia collaboration, 2018). The mean and the standard deviation of the residuals after the adjustment are respectively 0.08 and 2.13 mas in AL direction (compared to 0.05 and 2.14 in (Gaia collaboration, 2018)). 96% of the AL residuals fall in the interval $[-5,5]$ mas and 53% are at sub-mas level. 98% of the AC residuals fall

in the interval [-800 800] mas.

4. CONCLUSION

The INPOP19a planetary ephemeris is available on the IMCCE website www.imcce.fr/inpop with different formats: spice, calceph and the old JPL binary. A detailed documentation is also provided.

5. REFERENCES

- Fienga, A., Avdellidou, C., Hanus, J., 2019, "Asteroid masses obtained with inpop planetary ephemerides", MNRAS , 3035.
- Kuchynka, P., Folkner, W. M., 2013, "A new approach to determining asteroid masses from planetary range measurements.", Icarus 222, pp. 243–253
- Folkner, W. M., Williams, J. G., Boggs, D. H., Park, R. S., Kuchynka, P., 2014, "The Planetary and Lunar Ephemerides DE430 and DE431", IOM-196:C1
- Gaia Collaboration, 2018, "Gaia Data Release 2. Observations of solar system objects", A&A 616, pp.A13.
- Lawson, C., Hanson, R., 1974, "Solving least squares problems", eds SIAM